

## A CALORIMETRIC STUDY OF PHASE EVOLUTION IN A WE43 Mg ALLOY

G. Riontino\*, D. Lussana and M. Massazza

Dipartimento di Chimica I.F.M. and N.I.S. Centre, Università di Torino, via P. Giuria, 9, 10125 Torino, Italy

A DSC investigation has been performed on a Mg–RE–Y–Zr (RE=rare earth) technical alloy WE43. Hardness trend during isothermal treatments has been correlated to the calorimetric traces evolution and to the forming  $\beta$  phases with its precursors. Oversaturation of solute elements occurs at temperatures higher than 150°C, on cooling at room temperature after the anneals. Activation energies, found under non-isothermal conditions on artificially aged samples, suggest a slow transformation velocity, while the hardness response is relatively fast.

**Keywords:** DSC, heat treatments, Mg alloys, phase transitions

### Introduction

The recent increasing demand of lightness in transport industry has stimulated renewed interest in magnesium alloys. Correlations between physico-chemical properties and structure modifications due to thermal treatments have overcome an initial empirical approach to the problem. Recently, some authors [1–3] have reported a detailed analysis of the precipitation sequence in some Mg-rare earth-based alloys. The relationship between the different phases forming on annealing a metastable matrix, their morphology and their composition have been discussed. More generally, the role of solute elements and lattice defects has been emphasized [4–7], and the necessity of a better knowledge of the phase transformation mechanisms has been evidenced. The comparison with the Al alloys, for which a wide data dissemination has been made, offers a chance for interesting improvements also in Mg alloys. To this aim, the recent results of innovative thermal treatments on aluminium alloys of technical interest have traced a promising way of investigation [8, 9]. Present authors have shown for some aluminium alloys that a systematic calorimetric study offers a unique opportunity in describing the phase transformations responsible for the observed variations of mechanical properties [10–12]. In this paper, the calorimetric technique in scanning conditions (DSC) has been adopted for the first time at our best knowledge on a Mg alloy. Aiming to investigate the phase transformations induced by thermal treatments, attention has been paid on a phenomenological description of the structural modifications and its relevance on the microhardness

trend. The paper wishes to demonstrate that a preliminary and systematic DSC study is a necessary condition for a useful and reproducible design of thermal treatments of a given composition.

### Experimental

Gravity-cast samples of WE43 alloy, provided by Teksid-Aluminum Getti Speciali, (Mg+Y 4.2 mass%, Nd 2.3 mass%, other rare earths 1 mass%, Zr 0.6 mass%) have been used for this research. The alloy has been investigated in two thermal states: water quenched at room temperature after solutioning at 525°C for 8 h (WQ in the following), and artificially aged at 250°C for 16 h after quenching (T6). Chemical analysis, made on the WQ sample by Inductively Coupled Plasma-Atomic Emission Spectrometer (ICP-AES), has evidenced that the composition has remained the same than the as-cast original material, within the experimental error. Here and in the following, a thin oxide layer has been removed by mechanical grinding, after each thermal treatment and before any measurement. Calorimetric scan have been performed on specimens about 40 mg in mass, with a TA-2010 apparatus under protective pure argon atmosphere. The instrumental contribution (zero line) was subtracted from the original data, by scanning at the same rate the empty cell [13]. Hardness tests have been performed with a Vickers microindenter with a load of 3 N on the same samples used afterwards for DSC measurements; the reported data are the average of five indentations. Isothermal treatments have been made in an air-circulating furnace with a protective Al foil.

\* Author for correspondence: giuseppe.riontino@unito.it

## Results and discussion

In a previous work [14], we have associated the calorimetric evolution of a WE43 alloy to the commonly accepted precipitation sequence in this material [1]. The sequence involves the formation of a  $\beta$  phase having a nominal composition  $Mg_3X$ , with  $X$ =rare earth and/or Y. Samples quenched after solutioning, and samples artificially aged have been examined at different scanning rates. Common features of the curves (reported here in Fig. 1 for clarity of exposition) were: a) an initial exothermic signal P1 assigned to an undifferentiated formation of the metastable phases  $\beta''$  and  $\beta'$  followed by b) their dissolution or partial reversion D1-D2 and c) the formation of an intermediate phase  $\beta_1$  (P2) preceding the stable phase  $\beta$  (P3).

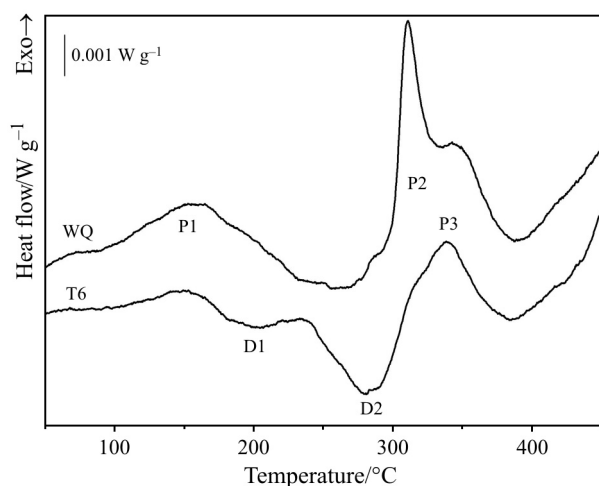


**Fig. 1** DSC traces, at  $2\text{ K min}^{-1}$ , of water quenched (WQ) and artificially aged (T6) WE43 samples. The labelled signals are discussed in the text

The main distinct features of the two samples are the different structuration of the endothermy and a substantial reduction of the signal P2 in the T6 sample. A different hardness value was also evidenced (71 vs. 86 VHN for WQ and T6, respectively). Aiming to detail the phase transformations responsible for the observed trends, isothermal treatments have been performed on quenched samples at temperatures suggested by the traces in Fig. 1.

### Evolution at 250°C

This is the temperature normally employed in the industrial practice [15]. Actually, it corresponds approximately to the temperature at which the first dissolution (signal D1 in the T6 sample) has been completed at the scan rate adopted. The DSC results are reported in Fig. 2a.

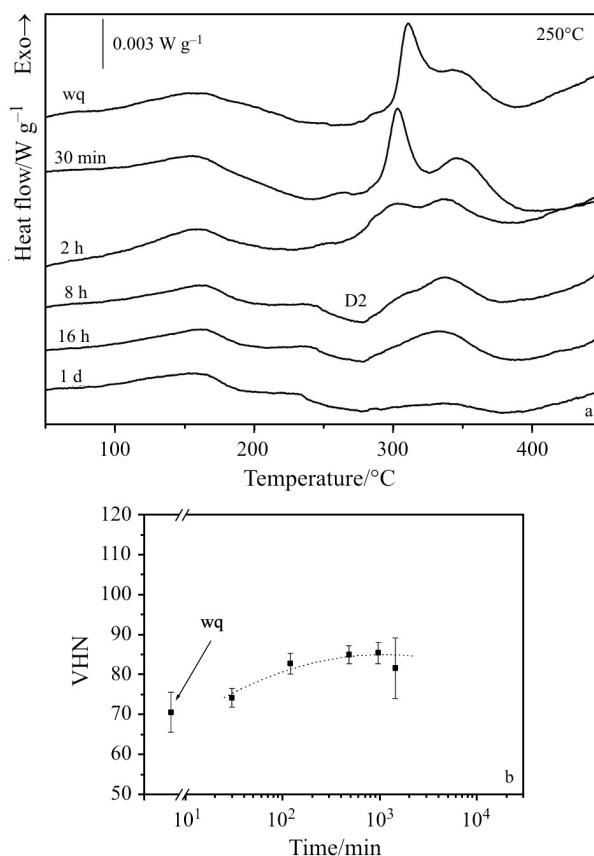


**Fig. 2** a – DSC evolution at 250°C, after quenching. The annealing time is labelled on each curve. Scanning rate:  $2\text{ K min}^{-1}$ , b – microhardness trend at 250°C: here and in the following the dotted line represents a guideline for the reader

The endothermic signal, undifferentiated in the as-quenched sample, becomes to separate into distinct contributions D1/D2 in the T6 sample. The first exothermic signal P1 remains substantially unchanged. The main signal P2 progressively disappears, like the signal P3 for the highest annealing times. The hardness (Fig. 2b) increases initially and finally stabilizes at a value 20% higher than the initial one. The conclusion can be drawn that the phase  $\beta'$  (whose dissolution during the calorimetric scan has been associated to the signal D2) has been at a large extent formed during the treatment at 250°C. The extended formation of  $\beta'$  justifies its enhanced transformation into  $\beta_1$  during the treatment, as hypothesized in [14]. Consequently, the signal P2 associated to the formation of  $\beta_1$  during the scan is reduced. The main contribution to the hardness increase is to be associated to the phases  $\beta'$  and  $\beta_1$ . When the formation of the stable phase  $\beta$  becomes to be important during the annealing at 250°C (with the consequent vanishing of the signal P3 on scanning), the hardness does not increase any more.

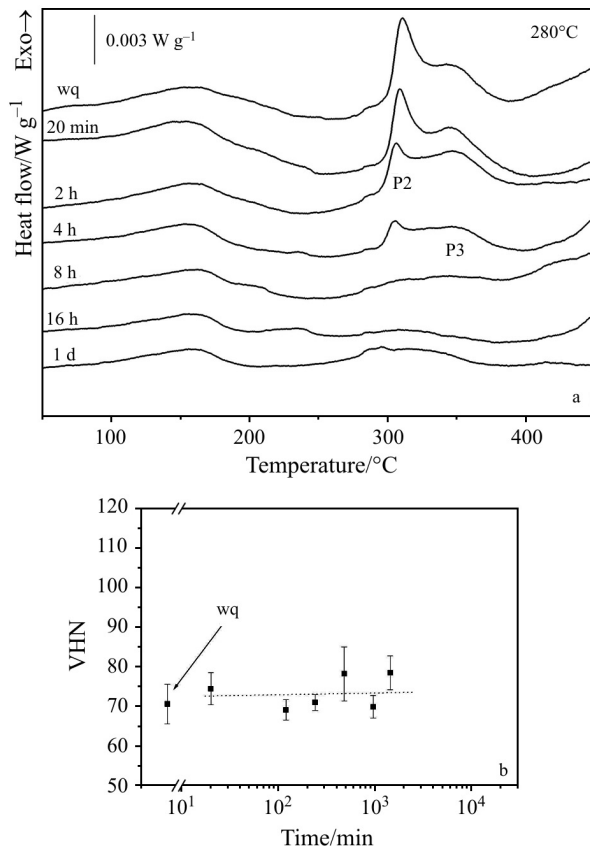


**Fig. 3** a – DSC evolution at 280°C, after quenching. The annealing time is labelled on each curve. Scanning rate: 2 K min<sup>-1</sup>, b – microhardness trend at 280°C

#### Evolution at 280°C

This temperature has been chosen to promote the main precipitation giving rise to the signals P2 and P3. At this temperature, in fact, the large dissolution signal D1-D2 in Fig. 1 is almost complete, and the main precipitation during the scanning has not yet occurred.

A substantial reduction of the dissolution signal with respect to the 250°C treatment, and in particular of the  $\beta'$  dissolution D2 (Fig. 3a), may be evidenced. This means that  $\beta''$  and  $\beta'$  have not formed during the annealing at 280°C. The formation of  $\beta_1$  (signal P2) is progressively reduced on scanning, like the formation of  $\beta$  (signal P3). The hardness does not change appreciably (Fig. 3b). At a first glance, one can suppose that the phase  $\beta_1$  has already formed during the isothermal treatment. This is apparently in contrast with the almost null increase of hardness (Fig. 3b), which normally benefits from the presence of  $\beta_1$ . A possible explanation arises from two considerations: 1) the formation of  $\beta_1$ , both during the annealing and on scanning, is difficult because  $\beta_1$  needs  $\beta''/\beta'$  to nucleate, but these last are strongly unstable at 280°C and vanish; 2) the few amount of  $\beta_1$  easily transforms in situ into  $\beta$

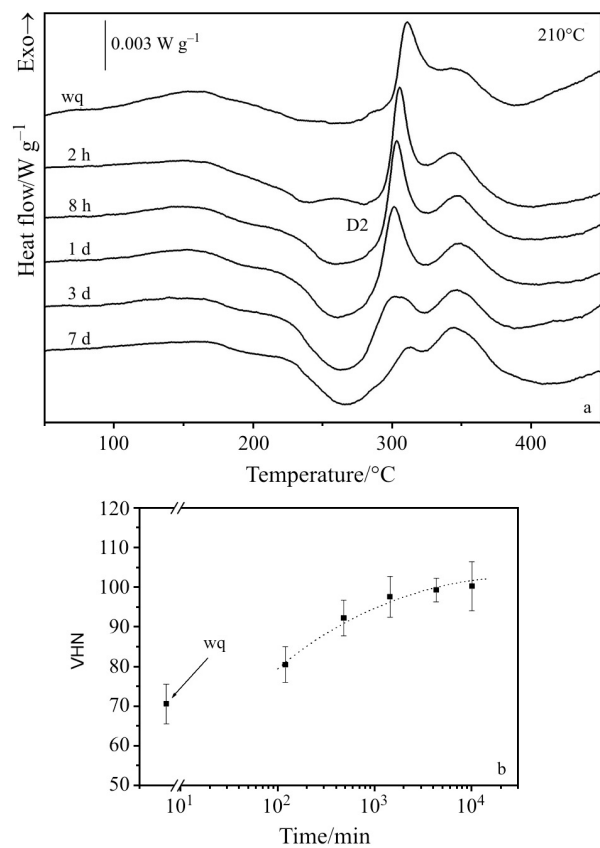


**Fig. 4** a – DSC evolution at 210°C, after quenching. The annealing time is labelled on each curve. Scanning rate: 2 K min<sup>-1</sup>, b – microhardness trend at 210°C

[2]. At this temperature the energy is sufficiently high to form almost directly the equilibrium phase  $\beta$  which does not contribute to increase the hardness.

#### Evolution at 210°C

The choice of this temperature has been suggested mainly by the feature of the large endothermic signal in Fig. 1. For the T6 sample, in fact, the contribution of the part D2 due to  $\beta'$  begins to be effective at around 250°C, when the dissolution of  $\beta''$  (D1) has just completed. Aiming to separate the two contributions to the subsequent phase transformations, the temperature of 210°C has been chosen, at which no  $\beta'$  dissolution has reasonably taken place. The resulting DSC traces and the microhardness trend are reported in Figs 4a and b, respectively.

Here again, the initial exotherm remains ( $\beta''$  and  $\beta'$  are forming during the scan), but it is more evident the  $\beta'$  formation on the annealing, centered on scanning at around 270°C. The presence of  $\beta'$  at the end of the thermal treatment leads again to a significant and rapid hardness increase up to the highest values found for our alloy, towards a plateau of about 100 VHN. The transformation  $\beta' \rightarrow \beta_1$  occurs only at the highest

annealing times, when by the reduction in amplitude of the signal P2 is visible. It doesn't further contribute to the hardness increase. It is interesting to note the small displacement of the signal P2 towards lower temperatures as the annealing time proceeds. This could be due to an enhanced facility of the  $\beta' \rightarrow \beta_1$  transformation as the  $\beta'$  formation itself is increased.

*Evolution at 150°C*

The above results show that whatever the annealing temperatures and times are, an initial and large exothermal signal P1 is always present on the successive scanning. This behaviour suggests that a certain degree of oversaturation is attained when the samples are cooled down at room temperature after the anneals. Hence, during the successive calorimetric scan, a certain amount of solutes form again precipitates, giving reason for the exothermic signal P1. A temperature must exist, at which this oversaturation is absent or reduced. On this basis, and considering the temperature range of the signal P1 in the previous figures, we have chosen 150°C for making thermal treatments, with the aim to possibly separate the concurrent phenomena that gives rise to the signal itself. The results are reported in Figs 5a and b.

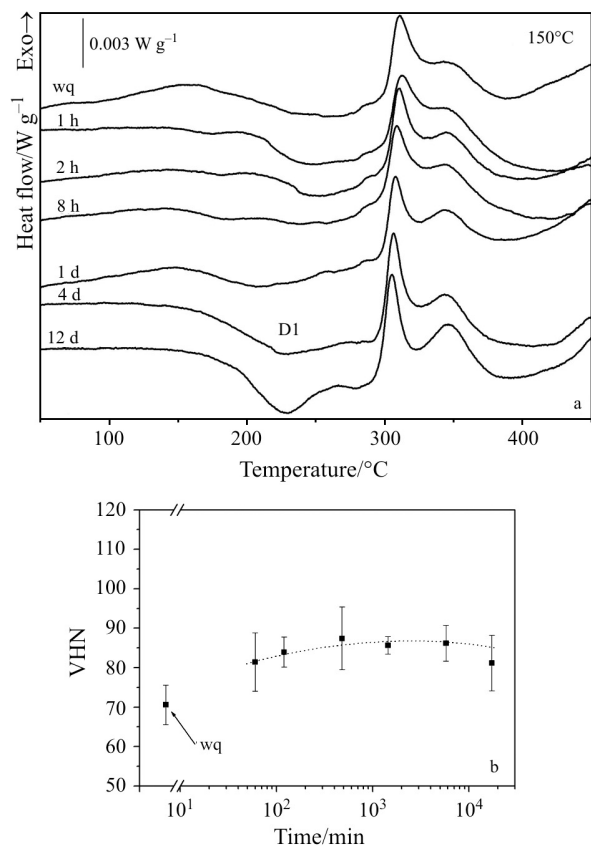


**Fig. 5** a – DSC evolution at 150°C, after quenching. The annealing time is labelled on each curve. Scanning rate: 2 K min<sup>-1</sup>, b – microhardness trend at 150°C

In effect, one can observe that the initial exothermic signal, still present after 1 day of treatment, tends to disappear after longer annealing times (Fig. 5a). This confirms that ageing at 150°C makes the oversaturation progressively reduced. In the same time, the contribution of  $\beta''$  dissolution increases on time, the  $\beta'$  dissolution does not change appreciably, and the main precipitation signal P2 and P3 remain unaltered. A different contribution of the two phases  $\beta''$  and  $\beta'$  has been in effect obtained. The hardness initially increases up to relatively high values, then remains stable or slightly decreases (Fig. 5b). The major contribution to the hardness increase is so given by  $\beta''$ . The DSC traces after the first annealing times (Fig. 5a) do not exclude that other calorimetric contributions could exist, but the instrumental sensitivity (together with the signals weakness) and the actual degree of comprehension of the phase transformations in age hardening Mg alloys do not allow any further consideration.

*Kinetic analysis*

The well defined separation of the calorimetric signals for the artificial aged sample T6 allows a kinetic analysis of the data to obtain the activation energies of the undergoing phenomena. For thermally activated phenomena, and without making any hypothesis on the mechanism which gives rise to a calorimetric signal, the logarithm of the scanning rate  $\Phi$  as a

**Table 1** Apparent activation energies in kJ mol<sup>-1</sup>

$\beta''$ dissolution	(signal D1)	172
$\beta'$ dissolution	(signal D2)	215
$\beta_1$ formation	(signal P2)	183
$\beta$ formation	(signal P1)	177

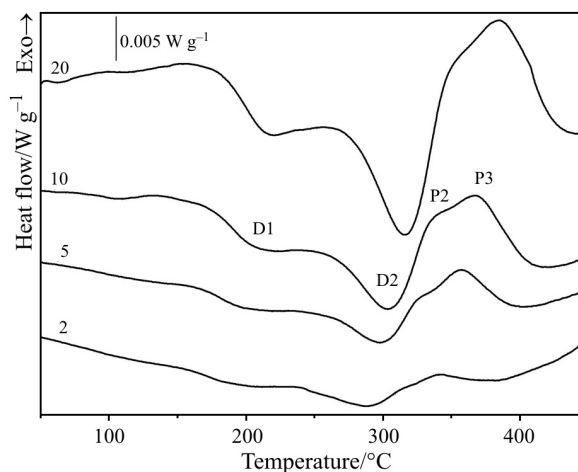


**Fig. 6** Calorimetric traces of a T6 sample at different scanning rates (labelled for each curve in K min<sup>-1</sup>)

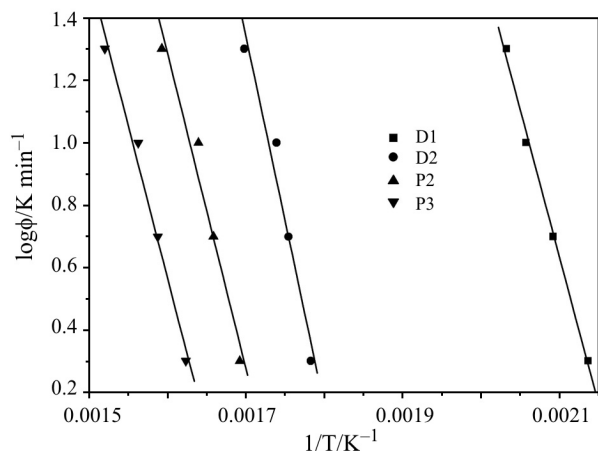


**Fig. 7** Log of scanning rate as a function of the reciprocal of the peak temperature of the signals in Fig. 6

function of the peak temperature displacement of each signal (Fig. 6) gives the results reported in Fig. 7. From the slope of the straight lines (Ozawa plot [16]), the apparent activation energies can be obtained. The results are reported in Table 1.

Few data exist in literature about the activation energies of such transformations. Pike and Noble [17], from electrical resistivity measurements on a dilute Mg–Nd alloy, obtain values for  $\beta''$ ,  $\beta'$  and  $\beta$  formation of the same order of magnitude than the present ones, and they tried to correlate the values with the vacancy assisted solute elements diffusion in the Mg matrix. The only consideration we can make is that the values here obtained are higher than the ones found in some Al alloys [18]. This could account for the slow kinetics of phase transformation commonly accepted for the Mg-rare earth-based alloys. Moreover, our hardness trends on annealing at different temperatures show a rather fast increase at short annealing times. This behaviour does not contrast with a relatively fast kinetic of formation of the hardening phases.

## Conclusions

Rather than exhaustive, since more direct observations seems necessary to give a paramount description of the phase transformation sequence, some considerations could be made from a systematic DSC investigation.

- A temperature has been individuated (150°C), over which a residual oversaturation of solute elements on cooling at room temperature after the annealing occurs.
- An annealing at 210°C is the most effective for increasing the hardness of the solid solution.

- A kinetic analysis under non-isothermal conditions suggests a slow velocity of the phase transformations responsible for the hardness trend. In the meantime, the initial hardness increase shows that the formation of the same phases is relatively fast.

## Acknowledgements

This work has been supported by a national project PRIN n. 2004023079. Thanks are due to M. Malandrino (Torino University) for chemical analysis and to A. Zanada (Teksid-Aluminum) for helpful discussions.

## References

- 1 C. Antion, P. Donnadieu, F. Perrard, A. Deschamps, C. Tassin and A. Pisch, *Acta Mater.*, 51 (2003) 5335.
- 2 P. J. Apps, H. Karimzadeh, J. F. King and G. W. Lorimer, *Scripta Mater.*, 48 (2003) 1023.
- 3 J. F. Nie and B. C. Muddle, *Acta Mater.*, 48 (2000) 1691.
- 4 J. F. Nie, in 'Viewpoint set n. 29: Phase transformations and deformations in Mg alloys', *Scripta Mater.*, 48 (2003) 981.
- 5 'Magnesium Alloys 2003', *Mater. Sci. Forum*, 419–422 (2003).
- 6 I. J. Polmear, overview 'Magnesium alloys and applications', *Mater. Sci. Technol.*, 10 (1994) 1.
- 7 P. Vostry, I. Stulikova, B. Smoula, M. Cieslar and B. L. Mordike, *Z. Metallkd.*, 79 (1988) 340.
- 8 R. N. Lumley, I. J. Polmear and A. J. Morton, *Intern. Patent Appl.*, PCT/WO 01/48259 A1 (2001).
- 9 R. N. Lumley, I. J. Polmear and A. J. Morton, *Mater. Sci. Forum*, 396–402 (2002) 893.
- 10 G. Riontino and M. Massazza, *Philos. Mag.*, 84 (2004) 967.
- 11 G. Riontino, S. Abis and P. Mengucci, *Mater. Sci. Forum*, 331–337 (2000) 1025.
- 12 G. Riontino, G. L. Ferro, D. Lussana and M. Massazza, *J. Therm. Anal. Cal.*, 82 (2005) 83.
- 13 W. F. Hemminger and S. M. Sarge, *J. Thermal Anal.*, 37 (1991) 1455.
- 14 G. Riontino, D. Lussana, M. Massazza and A. Zanada, *J. Mater. Sci. Letters*, in press.
- 15 Magnesium Elektron, Technical Sheet n. 467, Manchester (England).
- 16 T. Ozawa, *J. Thermal Anal.*, 2 (1970) 301.
- 17 T. J. Pike and B. Noble, *J. Less Common Metals*, 30 (1973) 63.
- 18 G. Riontino, S. Abis and C. Bottero, *Proc. 6<sup>th</sup> Intern. Conf. on Aluminum Alloys*, Toyohashi (Japan), 2 (1998) 903.

Received: August 31, 2005

Accepted: November 20, 2005

DOI: 10.1007/s10973-005-7125-6